

## Direct observation of energy-gap scaling law in CdSe quantum dots with positrons

M. H. Weber,<sup>1</sup> K. G. Lynn,<sup>1,2</sup> B. Barbiellini,<sup>3</sup> P. A. Sterne,<sup>4</sup> and A. B. Denison<sup>5</sup>

<sup>1</sup>Department of Physics, Washington State University, Pullman, Washington 99164-2814

<sup>2</sup>Center for Materials Research, Washington State University, Pullman, Washington 99164-2711

<sup>3</sup>Northeastern University, Boston, Massachusetts 02115

<sup>4</sup>Lawrence Livermore National Laboratory, Livermore, California 94551

<sup>5</sup>Idaho National Engineering and Environmental Laboratory, Bechtel BWXT Idaho, LLC, P.O. Box 1625, Idaho Falls, Idaho 83415

(Received 7 February 2002; revised manuscript received 28 May 2002; published 19 July 2002)

CdSe quantum dot samples with sizes in the range of 1.8–~6 nm in diameter were examined by positron annihilation spectroscopy. The results were compared to data obtained for single-crystal bulk CdSe. Evidence is provided that the positrons annihilate within the nanospheres. The annihilation line shape shows a smearing at the boundary of the Jones zone proportional to the widening of the band gap due to a reduction in the size of the quantum dots. The data confirm that the change in the band gap is inversely proportional to the square of the quantum dot diameter.

DOI: 10.1103/PhysRevB.66.041305

PACS number(s): 78.70.Bj, 41.75.Fr, 68.65.Hb, 73.21.La

The advent of reliable production of nanostructures has opened a different frontier in materials science. Quantum dot structures gain ever-increasing importance in applications ranging from semiconductor electronics to biological applications.<sup>1–3</sup> In order to take full advantage of this range of solids between molecules and macroscopic samples a detailed understanding of their electronic properties is essential. A wide range of techniques has been used towards this goal, many of which probe the electronic density of states. Here, we report on the application of positron annihilation spectroscopies, which provide information on the electron momentum distribution. A positron annihilates with an electron producing predominantly two  $\gamma$  ray photons of 511 keV, which are Doppler shifted by the combined momentum of the electron-positron pair. The positron reaches thermal equilibrium with its environment orders of magnitude faster than its typical lifetime in matter (several hundred picoseconds). While the electrons fill up energy levels in accordance with the Pauli principle, the sole positron is free to occupy its ground state. The intensity of modern positron beams is so low ( $\leq 10^6$  per second) that no more than one positron will reside in a quantum dot at any given time. Hence the examination of the Doppler shifts of the annihilation radiation will provide information about the electron momentum distribution in a sample. It is therefore not surprising that the positron annihilation Doppler broadening technique is exquisitely sensitive to changes in the electron structure as a function of size of the nanostructures.

Earlier measurements by Nagai, *et al.*<sup>4,5</sup> have shown possible evidence of quantum confinement for a distribution of sizes of Cu precipitates in Fe-Cu alloys. Xu *et al.* carried out studies for gold nanoprecipitates embedded in MgO that also showed some indication of this behavior.<sup>6</sup> However, the present study on CdSe quantum dots is the clear demonstration of size dependent effects. This work demonstrates that at least for select materials, positrons do indeed annihilate from within the quantum structures and that a size dependent signature is imprinted onto the annihilation radiation. We show that the band gap is inversely proportional to the square of the diameter of the quantum dots.

The measurements were conducted on spheres of 6 nm, 4.4 nm, 3.6 nm, 2.5 nm, and 1.8 nm diameter with a size distribution of about 12%. These spheres were prepared in the laboratories of Alivisatos (UC, Berkeley) and Bawendi (MIT). The production of CdSe quantum dots using colloidal precipitation from an organic solution is well established.<sup>7</sup> Growth is terminated when a coating of trioctylphosphine oxide (“TOPO,” ~1 nm) is formed. The size of all samples and their size distribution was determined using optical absorption spectra through the well-established wavelength dependence on size.<sup>8,9</sup> The sample material was dissolved in chloroform and then deposited on glass slides or polished silicon wafers. A single crystal of CdSe was examined as a reference sample. This crystal was annealed and subsequently etched in a 5% bromine methanol solution.

Monoenergetic positrons were implanted with kinetic energies between 1 and 5 keV depending on the thickness of the respective sample. Under these conditions more than 99% of the positrons are implanted in the layer of quantum dots. The energies of both annihilation photons were collected with two high-efficiency germanium detectors positioned on opposite sides of the sample and operated in coincidence.<sup>10–13</sup> The sum of the annihilation-photon energies ( $\Sigma E$ ) is a Doppler-free measurement of the rest mass of the electron-positron pair less the electron binding energy ( $\Sigma E = 2m_e c^2 - E_b \approx 2m_e c^2 = 1022$  keV). The difference in the photon energies is proportional to the momentum of the annihilating electron parallel  $p_{||}$  to the direction of photon emission ( $\Delta E \propto \vec{p}_{||} \vec{c} \approx$  keV). The use of two detectors in coincidence rather than one detector raises the signal to noise ratio from about 1000 to  $10^6$ . At the same time the energy resolution of the system degrades by  $\sqrt{2}$  (in the case of identical detectors), while the full Doppler shift is measured as opposed to only half when one detector is used only. Thus, effectively the energy resolution is improved. In this measurement the effective full width at half maximum energy resolution is 1.6 keV. Here, only the events with a sum energy within a 5-keV energy window of 1022 keV were used and accumulated as a function of the difference in the energy

of the photons. This measurement of the distribution of Doppler shifts gives the information about changes in electronic momentum structure occurring in these CdSe quantum dots in the quantum-confined regime.

The momentum distribution of valence and conduction electrons for a noninteracting electron gas in an ideal conductor leads to an annihilation Doppler line shape of an inverted parabola convoluted with the detector resolution. The parabola intersects zero at a momentum equivalent to the Fermi momentum (or radius). In spite of the repulsive interaction of positrons and ion cores a small fraction of positrons will annihilate with electrons from bound atomic states. These events add a much broader component to the spectrum with a momentum distribution that is specific for the chemical type of the element.

Semiconductors, of course, have a band gap of forbidden energies that modifies the electron momentum distribution. The Jones-zone model for semiconductors,<sup>14</sup> which gives a constant occupation of momentum states within the Jones zone and zero outside, yields an overall correct picture for the valence momentum density but an unphysical metallic behavior (i.e., sharp momentum cutoffs near the Fermi momentum for the valence electrons). In reality the opening of a band gap of forbidden energies produces a smearing of the sharp occupation breaks at the Jones-zone boundary. The width of this smearing is proportional to the energy gap.<sup>15</sup> In the quantum dots, the width of this smearing is expected to increase as the size becomes comparable to the Fermi wavelength, as is the case here. Friedel and Peter<sup>16</sup> provided an elegant discussion of the impact of the energy-gap widening in momentum space for a one-dimensional case, which can be extended in a straightforward manner to include the present case. Their formula indicates that the variation of the gap is proportional to the variation of the momentum density smearing width. Their ideas were inspired by work of Berko and Plaskett.<sup>17</sup>

In practice, the small reduction of occupied states in momentum space below the Fermi momentum is nearly impossible to observe. Above the Fermi momentum, on the other hand, the increase in occupied states results in intensity changes that are comparable to the intensity of annihilation events due to core electrons. To make this variation visible we have normalized the data from quantum dots to data from a bulk CdSe single crystal at each point in momentum space. The smearing out in momentum space and hence in Doppler shifts is most prominent at the Fermi momentum and leads to a peak in the normalized data. The normalized “ratio” curves shown in Fig. 1 show peaks at about 1.2 atomic momentum units (a.u.) on top of a gradually decreasing Gaussian-like function. With decreasing size of the quantum dots these peaks increase in area and shift to higher momentum. The area and centroid of these peaks were evaluated by fitting two Gaussians to the data in the region from 0 to 2.4 a.u. The first, centered at 0 a.u. tracks the gradual change and the second is fitted to the peak near 1.2 a.u. As an example, the fit to the 1.8-nm dot ratio is shown in Fig. 1. The centroid momenta of the peaks are shown as small bars.

The peak area is plotted in Fig. 2 as a function of quantum dot radius  $r$ . Also shown is a fit of a  $1/r^2$  dependence plus a

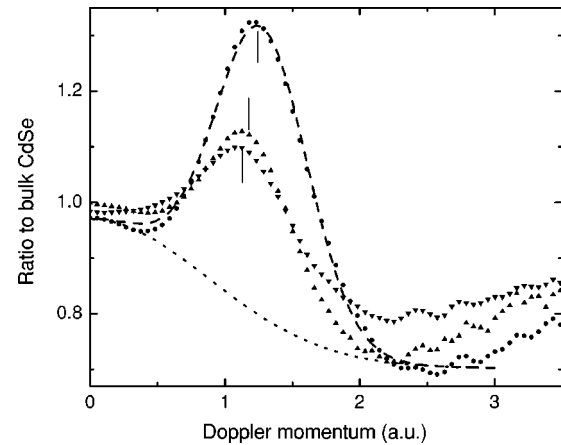


FIG. 1. Ratio of annihilation line-shape data for CdSe quantum dots (QD) of different sizes relative to bulk crystalline CdSe as a function of the Doppler momentum. The quantum dot sizes are 1.8 nm (large dots), 4.4 nm (up triangle), and 6 nm (down triangle). The small dot line is the central Gaussian fitted to the underlying ratio and the dashed line the two Gaussian fit to the peak and underlying ratio. Both are for the case of the 1.8 nm QD sample. Fits to the other samples are of similar quality. The vertical bars indicate the location of the centroid of the peaks (from fit).

constant offset to the area data. Wang and Zunger<sup>18</sup> performed electronic structure calculations for CdSe quantum dots and predicted a widening of the band gap as a function of dot radius. The same data are shown in Fig. 3 along with the centroid momentum of the peaks versus the nonexcitonic energy gap given by Wang and Zunger for quantum dots of nearly the same size. The linear relation is striking. It is evident that the centroid shift is a direct measure of the momentum smearing  $\Delta p$ , which is proportional to the energy-gap variation  $\Delta E$ . This is the first direct observation of a widening in the energy gap by positron annihilation. The centroid of the peak should also be proportional to the energy

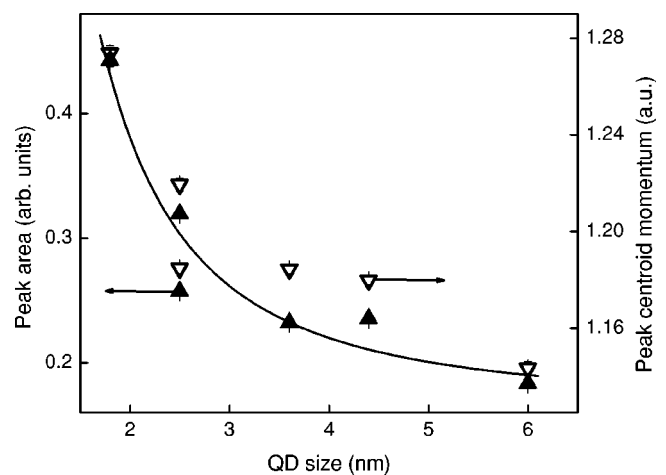


FIG. 2. Peak area (solid up triangles; left scale) and centroid momentum (open down triangles; right scale) versus the mean diameter of the quantum dots in the sample. An inverse square dependence fit of the area on the diameter is shown (solid line; left scale).

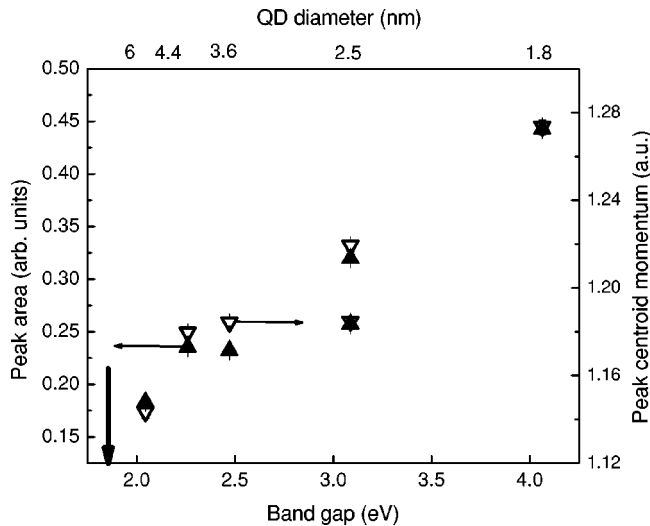


FIG. 3. Peak area (solid up triangles; left axis) and centroid (open down triangles; right axis) versus the band gap energy given by Wang and Zunger in Ref. 18. The arrow points to the bulk crystal band-gap energy estimate as extrapolated from the size dependency.

gap as shown in the figure. It should be noted that other models might yield different size dependencies. Saniz<sup>19</sup> suggested a  $1/r$  dependence. To test this, fits of  $1/r^n$  functions with  $n=1$ , and  $n=2$  were performed. The best  $\chi^2$  was obtained for  $n=2$ .

If the fit is extrapolated to infinite-size quantum dots (i.e., bulk crystals) the constant offset remains. This value can then be used to extrapolate the correlation of the peak area and center, respectively, to estimate the band-gap energy for bulk crystals. Given the uncertainties in the data, only a rough estimate of  $1.85 \pm 0.10$  eV can be given. This value is impressively close to the measured band-gap energy for CdSe of 1.77 eV at 300K (the data were collected at room temperature). Several factors can contribute to differences. The effective mass for positrons in a sample tends to be much larger than that for electrons. And finally the coupling of phonons to the positron can contribute on the order of tens of percent as calculated by Mikeska for metals, for example.<sup>20</sup>

Because of the small size of the nanospheres, it is possible that a significant fraction of the positron density could extend outside the spheres. Therefore, we performed calculations based on the density-functional theory<sup>21</sup> to describe positron wave functions and annihilation probabilities in CdSe. These calculations provide reliable predictions of positron affinities and annihilation rates.<sup>22–24</sup> Using a linear muffin-tin orbital (LMTO) basis set and the generalized gradient approximation (GGA) correlation potential we find that almost 80% of the positron wave function is confined to the interstitial region thus limiting the fraction that could extend beyond the quantum dot volume. The agreement between theory and the bulk CdSe data is reasonable in general and particularly good at the high-momentum region caused by core electron annihilations. The overlap between the valence electrons with the positron wave-function is expected to remain rather constant in the quantum dots. A small change in the positron wave-

function, due to the different boundary conditions in the quantum dots, can decrease the overlap with the core electron and might explain the changes in the ratio curves (Fig. 1) near zero momentum.

The quantum dots are coated with “TOPO,” which contains phosphorous. If the positron wave function has significant overlap with the TOPO region, a signature due to phosphorous would be present. The elemental signature from electrons bound to phosphorous has been observed in earlier experiments<sup>25</sup> in the form of a peak at 1.32 a.u. at a higher momentum than the peak observed here and this peak would show no size dependence. The ratio of phosphorous compared to bulk CdSe results in a monotonous decrease in the 1–2 a.u. momentum region and no peak.

Moreover, the calculations for the positron affinity for CdSe, following the method in Refs. 22,23, indicate that the positron cannot escape from CdSe and its nanoparticles. The positron affinity  $A$  is given by  $A = -(\phi^+ + \phi^-)$ , where  $\phi^+$  and  $\phi^-$  are, respectively, the work functions of the positron and electron. Using the experimental electron work function<sup>26</sup>  $\phi^- = 6.62$  eV and the theoretical positron affinity ( $-9.0$  eV) based on the LMTO calculations, the positron work function can be deduced as  $\phi^+ = -A - \phi^- = 2.2$  eV. Since  $\phi^+$  is positive, thermalized positrons cannot be emitted from the CdSe surface. Additionally, the positronium work function  $\phi^{Ps} = -A - 6.8$  eV (the binding energy of positronium) is also positive, indicating that positrons cannot be emitted from a CdSe sample either as free positrons or as positronium.

The reliability of the positron affinity calculation can be studied. The local-density approximation (LDA) shows a clear tendency to overestimate the magnitude of  $A^+$ , which can be traced back to the screening effects. In the GGA, the value of  $A^+$  is improved with respect to experiment by reducing the screening charge. For example, Kuriplach *et al.*<sup>27</sup> calculated  $A^+$  for different polytypes of SiC and showed that the GGA agrees better with the experimental values than the LDA. The computed  $A^+$  values in SiC depend also significantly on the quality of the wave-function basis set.<sup>28</sup> Interestingly, the result without atomic approximation and within GGA gives  $-3.92$  eV for 3C-SiC, which is close to the experimental value  $-3.83 \pm 0.45$  eV.<sup>29</sup> In the case of CdSe we tried GGA-LMTO calculations with different sphere sizes to describe the interstitial region. These resulted in comparable positron affinities. Therefore from these calculations we can conclude that the uncertainty of our result is smaller than 1 eV and therefore smaller than the positron work function.

A recent addition to this work is the ability to measure positron lifetimes. The construction of the lifetime setup in the target area of the beam is a nontrivial task yet such lifetime measurements provide further support that the positron overlap with the electron density remains fairly constant as a function of the dot size. The lifetime of positrons implanted into bulk CdSe with 2 keV was measured. An experimental lifetime of 275 ps was found in excellent agreement with the theoretical value of 279 ps based on the GGA theory,<sup>22,23</sup> indicating that our bulk sample is of good quality (without any significant concentration of atomic point defects). The corresponding lifetime measured in the 6-nm CdSe sphere

was 251 ps, which is very close to the bulk value. Moreover, the existence of positronium, the positron-electron bound state would give a lifetime component in the spectra of 1 ns or greater. The contribution of this lifetime component is less than 1.3% indicating positronium does not exist within the CdSe quantum dot or at its surface. Further studies are being carried out measuring the lifetime in the smaller quantum structures.

In summary, our results indicate the utility of the positron annihilation technique as a sensitive probe of the electronic structure and momentum density in semiconductor quantum structures. We have observed directly the widening of the electronic band gap as the quantum dot size decreases. The implications of these observations are significant in that a simple spectroscopic measurement with positrons can reveal

detailed information on mesoscopic systems. The measurement of the angular correlation of the annihilation photons allows for a direct observation of the electron momentum distribution in quantum dots. Here we confirm, that, at least in the case of CdSe quantum dots, positron annihilation occurs from within the quantum structures.

This work was supported by the Department of Energy Division of Materials Sciences, Condensed Matter Physics branch under Contract No. DE-AC07-00ID13727 (INEEL), Grant No. DEFG0301ER45866 (WSU), and US DOE Contract No. W-31-109-ENG-38, and benefited from the allocation of supercomputer time at the Northeastern University Advanced Computation Center (NU-ASCC). The authors greatly appreciate the generous donations of samples from A.P. Alivisatos (UC, Berkeley) and M.G. Bawendi (MIT).

- 
- <sup>1</sup>G.L. Timp, *Nanotechnology* (AIP Press, New York, Inc./Springer-Verlag, New York, 1998).
- <sup>2</sup>P. Harrison, *Quantum Wells, Wires and Dots* (Wiley, New York, 1999).
- <sup>3</sup>H. Mattoussi, J.M. Mauro, E.R. Goldman, G.P. Anderson, V.C. Sundar, F.V. Miculec, and M.G. Bawendi, *J. Am. Chem. Soc.* **122**, 12 142 (2000).
- <sup>4</sup>Y. Nagai, M. Hasegawa, Z. Tang, A. Hempel, K. Yubuta, T. Shimamura, Y. Kawasoe, A. Kawai, and F. Kano, *Phys. Rev. B* **61**, 6574 (2000).
- <sup>5</sup>Y. Nagai, T. Chiba, Z. Tang, T. Akahane, T. Kanai, M. Hasegawa, M. Takenaka, and E. Kuramoto, *Phys. Rev. Lett.* **87**, 176402 (2001).
- <sup>6</sup>J. Xu, A.P. Mills, Jr., A. Ueda, D.O. Henderson, R. Suzuki, and S. Ishibashi, *Phys. Rev. Lett.* **83**, 4586 (1999).
- <sup>7</sup>X.G. Peng, M.C. Schlamp, A.V. Kadavanich, and A.P. Alivisatos, *J. Am. Chem. Soc.* **119**, 7019 (1997).
- <sup>8</sup>C.B. Murray, D.J. Norris, and M.G. Bawendi, *J. Am. Chem. Soc.* **115**, 8706 (1993).
- <sup>9</sup>I.E. Brus, A.L. Efros, and T. Itoh, *J. Lumin.* **70**, R7 (1996).
- <sup>10</sup>K.G. Lynn, J.R. MacDonald, R.A. Boie, L.C. Feldman, J.D. Gabbe, M.F. Robbins, E. Bonderop, and J.A. Golovchenko, *Phys. Rev. Lett.* **38**, 241 (1978).
- <sup>11</sup>P. Asoka-Kumar, M. Alatalo, V.J. Ghosh, A.C. Kruseman, B. Nielsen, and K.G. Lynn, *Phys. Rev. Lett.* **77**, 2097 (1996).
- <sup>12</sup>M. Alatalo, H. Kauppinen, K. Saarinen, M.J. Puska, J. Mäkinen, P. Hautojärvi, and R.M. Nieminen, *Phys. Rev. B* **51**, 4176 (1995).
- <sup>13</sup>K. Saarinen, J. Nissilä, H. Kauppinen, M. Hakala, M.J. Puska, P. Hautojärvi, and C. Corbel, *Phys. Rev. Lett.* **82**, 1883 (1999).
- <sup>14</sup>A. MacKinnon, and B. Kramer, *J. Phys. C* **13**, 37 (1980).
- <sup>15</sup>E.D. Isaacs and P. Platzman, *Phys. Today* **49** (2), 40 (1996).
- <sup>16</sup>J. Friedel and M. Peter, *Europhys. Lett.* **8**, 79 (1989).
- <sup>17</sup>S. Berko, J.S. Plaskett, *Phys. Rev.* **112**, 1877 (1958).
- <sup>18</sup>L.W. Wang and A. Zunger, *Phys. Rev. B* **53**, 9579 (1996).
- <sup>19</sup>R. Saniz (private communication).
- <sup>20</sup>H.J. Mikeska, *Phys. Lett.* **24A**, 402 (1967).
- <sup>21</sup>M.J. Puska and R.M. Nieminen, *Rev. Mod. Phys.* **66**, 841 (1994).
- <sup>22</sup>B. Barbiellini, M.J. Puska, T. Torsti, and R.M. Nieminen, *Phys. Rev. B* **51**, 7341 (1995).
- <sup>23</sup>B. Barbiellini, M.J. Puska, T. Korhonen, A. Harju, T. Torsti, and R.M. Nieminen, *Phys. Rev. B* **53**, 16 201 (1996).
- <sup>24</sup>B. Barbiellini, M. Hakala, M.J. Puska, R.M. Nieminen, and A.A. Manuel, *Phys. Rev. B* **56**, 7136 (1997).
- <sup>25</sup>M.P. Petkov, M.H. Weber, K.G. Lynn, R.S. Crandall, and V.J. Ghosh, *Phys. Rev. Lett.* **82**, 3819 (1999).
- <sup>26</sup>A.H. Nethercot, *Phys. Rev. Lett.* **33**, 1088 (1974).
- <sup>27</sup>J. Kuriplach, M. Sob, G. Brauer, W. Anwand, E.-M. Nicht, P.G. Coleman, and N. Wagner, *Phys. Rev. B* **59**, 1948 (1999).
- <sup>28</sup>B. Barbiellini, J. Kuriplach, W. Anwand, and G. Brauer, *MRS Proc. Fall 2000* **640**, 249 (2001).
- <sup>29</sup>B.K. Panda, G. Brauer, W. Skorupa, and J. Kuriplach, *Phys. Rev. B* **61**, 15 848 (2000).